Synthesis of nano-structured Duplex and Ferritic stainless steel powders by planetary milling: An experimental and simulation study

This thesis is submitted in the partial fulfillment of the requirement
for the Bachelor & Master degree of Technology in
Metallurgical and Materials Engineering

By

SHALABH GUPTA

(710MM1169)

Under the guidance of

Prof. D. Chaira

NATIONAL INSTITUTE OF TECHNOLOGY, ROURKELA

NATIONAL INSTITUTE OF TECHNOLOGY, ROURKELA

CERTIFICATE

It is to certify that the thesis submitted by Shalabh Gupta which is entitled as "Synthesis of nano-structured Duplex and Ferritic stainless steel powders by planetary milling: An experimental and simulation study" which is in partial fulfillment of the requirements for the award of Masters in Technology degree in Metallurgical and Materials Engineering at the National Institute of Technology, Rourkela, is an authentic work which is carried out by him under my guidance and supervision.

The matter contained in the thesis has not been submitted to any other University/institute for the award of any degree or diploma.

Date: 21th May, 2015

Dr. D Chaira

Department of Metallurgical

and Materials Engineering

National Institute of Technology,

Rourkela-769008

ACKNOWLEDGEMENT

I wish to pay my sincere thanks and gratitude to Prof. S.C Mishra, Head of the Department, Metallurgical and Materials Engineering, NIT Rourkela for providing me an opportunity to work on the given project and provide me the departments' valuable resources

With immense pleasure, I would would be willing to express my deep sense of gratitude and indebtness to my guide, Prof. D. Chaira, Department of Metallurgical and Materials Engineering, NIT Rourkela, for his fruitful and valuable guidance, consistent encouragement and kind support throughout the year and his inputs in the execution of the dissertation work.

I convey my regards to Mr. Shashanka R., research scholar, Department of Metallurgical and Materials Engineering, NIT Rourkela, for his timely support and effective guidance at the time of the project work.

Date: 21th May, 2015

Shalabh Gupta

(710MM1169)

Department of Metallurgical

and Materials Engineering,

National Institute of Technology,

Rourkela, 769008

ABSTRACT

Nano-structured duplex and ferritic stainless steel powders were prepared by planetary milling of elemental Fe, Ni and Cr powder compositions (duplex: 69Fe-18Cr-13Ni and ferritic:82Fe-17Cr-1Ni) in a dual drive planetary mill for 10 hours. The feasibility for solid solution formation of Cr and Ni in Fe matrix were studied. The samples were collected at regular time intervals and characterized for their morphological and phase analysis using X-Ray diffraction (XRD) and scanning electron microscopy (SEM). It has been observed that as the milling time increases crystallite size decreases and lattice strain increases. Powders were then compacted and sintered at the temperature of 1000 °C with a holding time of 1 hour. The sintered samples were again characterized for their morphological and phase change analysis using same techniques.

Thermodynamic aspects of milled stainless steel powders were performed using Miedema model. The theoretical values of ΔH, ΔS and ΔG were calculated and found to be -14.32kJ/mol, 6.93J/mol and -16.39 kJ/mol for duplex stainless steel and -2.81kJmol, 4.35Jmol and -4.11 kJ/mol for ferritic stainless steel respectively. The thermodynamic parameters were further experimentally calculated by differential scanning calorimetry (DSC) and the value of ΔH was found to be -174.9 kJ/mol for duplex stainless steel and -134.2 kJ/mol for ferritic stainless steel respectively.

Keywords: Stainless steel; planetary milling; Miedema model; thermodynamic parameters

List of Figures

Fig. 12	Optical microstructure of (a) duplex stainless steel and (b) ferritic stainless steel samples sintered at 1000°C for1 h
Fig. 13	SEM images of compacted powders of (a) duplex (b) ferritic stainless steel and 1 wt. % Yittria strengthened (c) Duplex and (d) ferritic stainless steel
Fig. 14	EDS spectra of 1 wt. % Yittria dispersed ferritic stainless steel

List of Tables

Contents

DISSEMINATION OF WORK

1. **Shalabh Gupta, R. Shashanka, D. Chaira* :** Synthesis of nano-structured duplex and ferritic stainless steel powders by planetary milling: An experimental and simulation study : *IOP Conf. Ser.: Mater. Sci. Eng.* **75** 012033 doi:10.1088/1757-899X/75/1/012033

2. R. Shashanka, D. Chaira, Phase transformation and microstructure study of nano structured duplex and ferritic stainless steel powder prepared by planetary milling, Powder Technol. 259 (2014) 125–136.

3. Shashanka. R, D. Chaira, Development of nano-structured duplex and ferritic stainless steels by pulverisette planetary milling followed by pressureless sintering, Materials Characterization 99 (2015) 220–229

Chapter 1
Introduction

1. Introduction

Preparation of stainless steel by powder metallurgy route has been the cause of much scientific attention because of its capability of manufacturing components with a diversified range of mechanical properties which have near-net shape by making use of different alloy selections and processing methods. Though powder metallurgy can be employed for various grades of stainless steel powder production but duplex and ferritic stainless steels among them have been extensively studied owing to the versatility of their applications.

Conventionally, duplex stainless steels are usually involved in orthopedic applications some which are surgical cutting tools or medical implants and applications where high toughness levels are required in compatibility with cryogenic applications as well as creep resistance [1]. Different processing methods are being adopted for improvement of the structure and properties of stainless steels. Methods such as equi-channel angular pressing, torsion at high pressure and mechanical alloying are being employed in order to attain structural refinement for both metals and alloys [2]. Among all of the mentioned methods, mechanical alloying proves to be one of the best powder metallurgy routes for refinement of the particle size to nano scale. Thus, specially designed dual drive planetary mill (DDPM) was used in order to synthesize nano-structured stainless steel. The high-energy milling synthesis route is one of the most promising synthesis method from the industrial perspective because it involves the use of comparatively less expensive equipment for the synthesis of nano-structured powder in bulk. In fact, it has numerous common aspects which includes mixing, finer grinding and comminution of materials. Alloy formation occurs due to diffusion at the time of planetary milling of elementary powder particles which results in atomic level alloying usually accompanied by nano sized structured meta-stable phase transformation [3–5]. The high density of dislocations and grain boundaries

formed in powders and micro segregation of solute at these defects may result in the formation of extended solid solutions [6]. Thermodynamic parameters play a very crucial role in order to predict the solid solution formation at the time of planetary milling. Very few literatures are available so far which studies the calculation of thermodynamic parameters for some of the binary systems such as Ti-Ni, Ti–Al, Al–Ni and Al–Ni–Ti by using Miedema model [7, 8]. In the present study, an attempt has been made to evaluate different thermodynamic parameters of ternary system (Fe-Ni-Cr) during planetary milling. Here, we primarily intend to predict various thermodynamic parameters during synthesis of nano-structured stainless steel by planetary milling.

Chapter 2

Literature Review

2. Literature Survey

2.1 Powder Metallurgy:

Powder metallurgy is a metal forming technology used to produce dense and precision components. Different routes for powder and component forming can be employed in order to create an end product with application specific properties for a particular industry. Recent advances in powder metallurgy studies a wide range of materials as well as techniques which uses powder metallurgy and use of this technology across a wide variety of application areas. The figure below shows different fields which uses powder metallurgy for fabrication of different components.

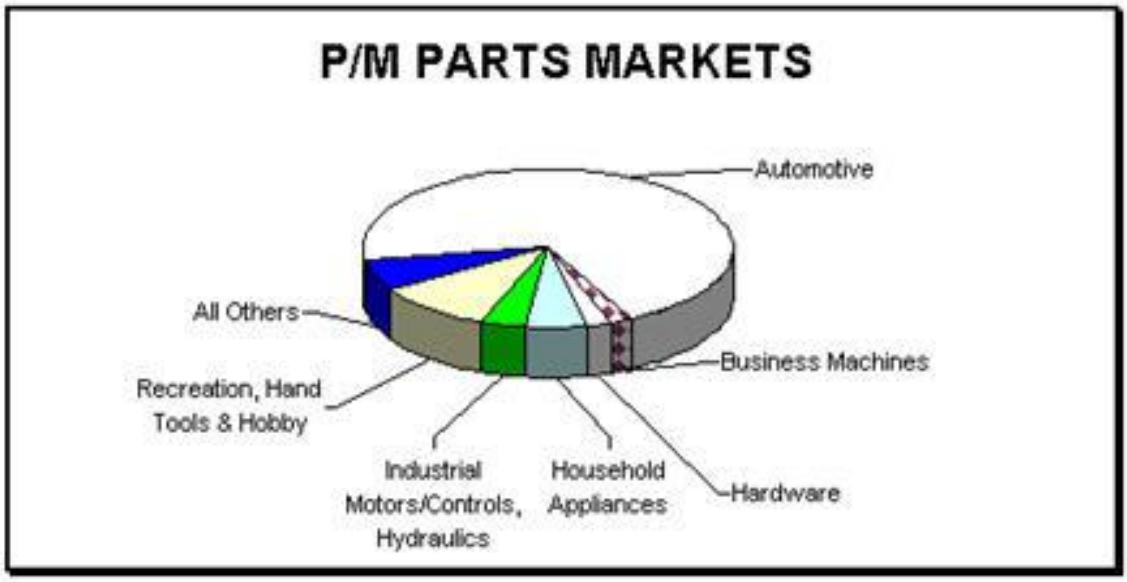

Fig. 1: Use of powder metallurgy in different market sectors

2.2 Mechanical Alloying:

Mechanical alloying (MA) is a powder processing technique which allows production of homogeneous materials starting from blended elemental powder mixtures. It is normally a dry, high-energy ball milling technique and has been employed to produce a variety of commercially useful and scientifically interesting materials. It was originally developed in order to produce oxide-dispersion strengthened (ODS) nickel-iron based super alloys which has a wide applications in aerospace industry, MA has also proved its efficiency to synthesize different varieties of equilibrium and non-equilibrium alloy phases originating from elemental or pre alloyed blend of powders. The non-equilibrium phases synthesized include supersaturated solid solutions, metastable crystalline phases and quasi crystalline phases, nanostructures, and amorphous alloys.

Usually materials at nano-range behave entirely different from their bulk form [9] and hence we prepared nanostructured duplex (Fe–18Cr–13Ni) and ferritic (Fe–17Cr–1Ni) stainless steel powders usinf mechanical alloying as one of the favorable method. Recent advances in these areas and mechanochemical synthesis of materials had been critically reviewed after the discussion of different processes and process variables involved in MA. The present understanding of modeling of the mechanical alloying process has also been discussed.

2.2.1 Different stages of Mechanical Alloying

Mechanical alloying can be sub classified into different stages, which are:

- Particle flattening: This is the initial stage of milling and initially the particles get flattened and become somewhat like flakes.

- Welding predominance: In the second stage the initially flattened particles weld together in order to form lamellar or layered composite particles.
- Equiaxed particle formation: After this, the lamellar particles become thicker and rounded from their previous flake like appearance. The work hardening of the powder causes the change in its shape
- Random welding orientation: Rewelding of particles starts as soon as the fragments from the equiaxed particles start welding in different orientations and their lamellar structure begins to degrade.
- Steady state processing: Finally, the material structure gets gradually refined as fragments are taken from the particles that weld later with other fragments in different orientations.

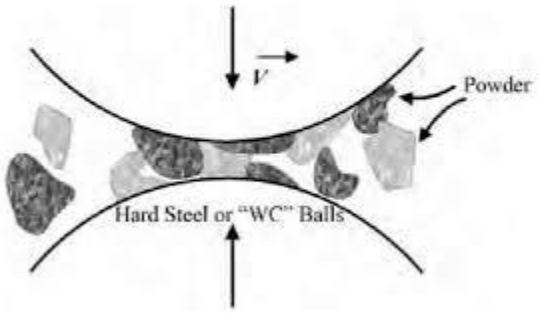

Fig. 2: Ball-powder-ball collision of powder mixture during reaction milling process [10]

2.2.2 Some attributes of Mechanical Alloying

- Grain refinement up to nanoscale
- Extension of solid solubility limits
- Producing dispersed second phase (i.e oxide usually) particles
- Synthesizing novel crystalline and quasi crystalline phases

- Developing amorphous (glassy) phases
- Disordering, ordered intermetallic
- Possibility of alloying elements which are difficult to alloy

2.2.3 Process of Mechanical Alloying

The most important components in MA:

- Raw Materials
- Ball Mill
- Types of Mill used
- Various Process variables

Mechanical alloying starts with mixing powders in required proportion followed by loading the powder mix into mill along with the medium required for grinding (generally steel balls). The blend thus obtained is milled for desired length time duration until a steady state is attained. Steady state is a state when the composition of every powder particle is homogenized such as that of the proportion of the elements in the initial powder blend. Followed by milling, the powder is consolidated into a bulk shape and then heat treated in order to get desired microstructure and properties [11].

Usually raw materials which have particle sizes lying between 1 and 2000nm are used in MA. The particle size of powder decreases exponentially with increase in time and attains a small value of few microns after a few minutes of milling. So, size of powder particle is not much critical, except that it should be comparatively smaller than the size of the grinding ball. The raw powders falls into broad categories of master alloys, pre-alloyed powders, pure metals and

refractory compounds. Dispersion strengthened materials contain additions of oxide, carbides and nitrides usually. Most common among them are oxides and such alloys are known as oxide-dispersion strengthened (ODS) alloys. In previous years, the powder blend was always composed of at least 15 vol. % of a ductile compressible deformable metal powder which acts as host or a binding element. However, in these recent years, blends composed of fully brittle material have been successfully milled leading to alloy formation. Thus, it is no longer necessary to have a ductile metal powder in the blend as a necessary component. Thus, brittle-brittle powder mixture are also milled in a similar fashion as that of ductile-ductile and ductile-brittle powder mixtures to produce novel alloys. Sometimes, metal powder particles are milled in a liquid medium which is known as wet grinding. Absence of any liquid medium for milling is known as dry grinding [12].

Cryomilling is also one of the kind of wet milling which uses liquid at cryogenic temperature. In such a case, the solvent molecules are adsorbed on the surfaces of the particles which are newly formed and thus lower their surface energy. Thus wet grinding is more preferable in comparison to the dry grinding to obtain finer grounded products. The less-agglomerated condition of the powder particles in the wet condition is also a useful factor. Faster amorphization in case of wet grinding has also been reported. But the chances of contamination of the powder particles increases due to sticking in case of wet grinding. Thus, usually MA/MM operations are mostly carried out in dry conditions [13]. Mechanical alloying/mechanical milling is carried out in ball mill. The general principle of ball milling operation is given below.

1. **Ball Mill:** A ball mill, a sort of processor, is a tube shaped device utilized as a part of crushing (or blending) materials like metals, chemicals, ceramic raw materials and paints.

Ball mill pivot around a hub which is pivot, halfway loaded with material which has to be ground in addition to the granulating medium. Diverse materials are utilized as media, including ceramic and stainless steel balls. A falling impact which is of inward orientation decreases the material to a fine powder. Modern industrial ball mills can work persistently, bolstered toward one side and released at the flip side. Huge to medium-sized ball factories are mechanically pivoted on their hub, yet small ones regularly comprise of a barrel shaped topped compartment that sits on two commute shafts (pulleys and belts are utilized to transmit rotating movement). A stone tumbler works on similar guidelines. Ball mills are likewise utilized as a part of fireworks and the production of black powder, however it cannot be utilized as a part of the readiness of some pyrotechnic mixtures, for example, flash powder due to their affectability to impact. High quality ball mills are conceivably expensive and can crush mixture particles which are as minute as 5 nm, immensely expanding surface area and rate of reaction. The grinding works on the principle of critical speed [13]. The critical speed can be seen as the speed after which the steel balls (which are in charge of the pounding of particles) begin pivoting along the bearing of the round and hollow device; causing no further crushing action. Ball mills are usually used as part of the mechanical alloying process in which they are utilized for crushing as well as for cold welding, aiming the purpose of generating alloys from the initially powders. The ball mill is a key equipment used for grinding crushed materials, and it is broadly utilized in production lines crushing powders, for example, concrete, silicates, recalcitrant material, fertilizer, glass, ceramics production, and so on and additionally for mineral dressing of both ferrous non-ferrous metals. The ball mill can crush different minerals and different materials either wet or

dry. There are two sorts of ball mill, grate sort and over fall sort because of distinctive methods for grinding material. There are numerous sorts of granulating media suitable for utilization in a ball mill, every material having its own particular properties and advantages. Key properties of grinding media are size, thickness, hardness, and composition [11].

a. Size: Smaller size of the media particles indicates smaller particle size of the end product. The grinding media particles should be substantially larger than the largest pieces of material to be ground.
b. Density: The grinding media should have higher density than the material being grounded.

   It becomes problematic if the grinding media starts floating on top of material to be ground.
c. Hardness: The grinding medium should have optimal properties of both enough durability so as to grind the material as well as appropriate value of toughness so that it does not wears down the tumbler at a faster pace.
d. Composition: Different grinding applications have different and specific requirements. Some of them are factually based on the point that there will be some of grinding media in the finished product. The others are based on how the media reacts to the material which is being ground.

- Where the color of end product is of due importance, the color as well as material of the grinding media must be considered.

- The case in which low contamination is must, the grinding media may be chosen from the perspective of ease of separation from the final product (e.g.: steel dust which is produced from stainless steel media can be easily separated from non-ferrous products through magnetic separation). As an alternative route, the grinding media shall be taken same as that of the material being grinded.
- Flammable products tend to become explosive in their powder form. Steel media may cause sparking, by becoming an ignition source for such products. For these samples, either wet-grinding or non-sparking media such as lead or ceramic shall be chosen.
- Media, such as iron, may have a tendency to react with corrosive materials. To avoid this, ceramic, stainless steel, and flint grinding media may each shall be used in the presence of corrosive substances during grinding.
- The grinding chamber can be filled with an inert gas which provide shielding effect and behaves inertly to the material being ground, to avoid oxidation or explosive reactions that may take place with ambient air filled inside the mill [11].

2.3 Types of Mill:

Different varieties of high-energy milling equipment are being used in order to produce mechanically alloyed powders. They have different capacity, mill efficiency and additional arrangements for cooling and heating etc.

Some of the mills are:

- SPEX shaker mill
- Planetary ball mill
- Attrition mill

- Commercial mill

SPEX Shaker Mill:

Shaker mills, are most commonly used for laboratory investigations and for alloy screening purposes, it can mill about 10–20 g of powder at a time. The most common variety of these mill has single vial, containing the sample as well as grinding balls, which are secured in clamp and are swung energetically back and forth some thousand times within a minute. The to-and-fro shaking movement is combined with lateral motion of the ends of vial, so that the vial appears to describe a figure 8 or infinity sign as it moves [14]. With every swing, the balls in the vial impact against the sample and the vial end, both mixing as well as milling the sample. Due to the amplitude (about 4-6 cm) and high speed (about 1300 rpm) of the clamp motion, the ball velocities are higher (on the order of 4-6 m/s) and consequently the force of ball's impact is unusually very large. Therefore, these mills can also be considered of high-energy variety [11]. The below shows a SPEX Shaker Mill.

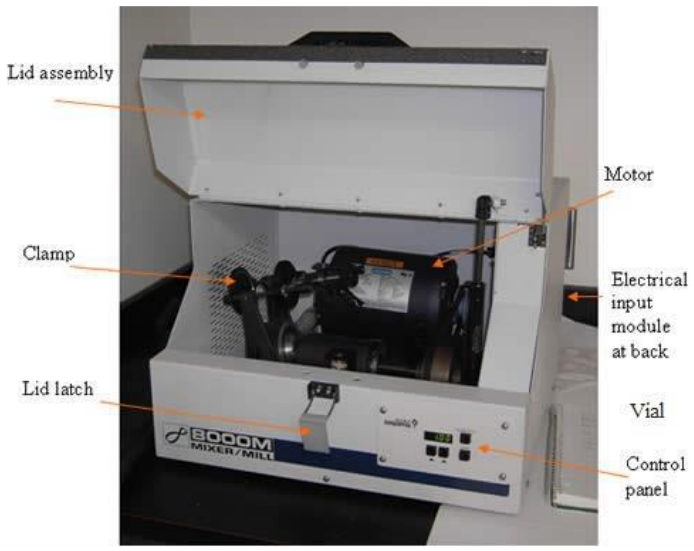

Fig. 3: SPEX Shaker Mill [8]

Planetary Ball Mill:

Planetary ball mill is capable of milling few hundred grams of the powder at a time. The planetary ball mill draws its name from the planetary movement of its vials. These vials have been arranged on a rotating supporting disk and a specialized driving mechanism causes their rotation around their own axes [11]. The centrifugal force which is produced by the rotation of the vials around their axes and that produced by the rotation of the supporting disk both acts on vial consents, comprising of grinding material and also the grinding balls. Since the vials and the support disk rotate in directions opposite to each other, the centrifugal forces act alternately in both like and opposite directions. This results in the grinding balls to run inside wall of the vial — the effect of friction, followed by material being ground and grinding balls lifting off and traveling freely through the inner chamber of vial and colliding against the opposition inside wall. The figure of a planetary ball mill is shown below.

Fig. 4: Dual drive Planetary Ball Mill

Attrition Mill:

Ball mill comprises of a rotating horizontal drum partially filled with small steel balls. The rotation of the drum causes the ball to drop on the metal powder which has to be grounded; the rate of grinding is directly proportional with the rotation speed. At higher speeds, however, the centrifugal force which acts on steel balls exceeds the gravitational force, and the balls gets pinned to the wall of the drum. At this juncture the grinding action ceases. An attritor (a ball mill which is capable of generating higher energies) comprises of a vertical drum containing a series of impellers in it [15]. These impellers are set progressively at right angles to one another. They energize the ball charged, causing reduction in powder size because of impact between balls, and the wall of the container, and in between balls, agitator shaft, and impellers. Some reduction in size takes place by the inter particle collisions and ball sliding. A powerful motor rotates the impellers, leading to agitation of the steel balls in the drum.

Attritors are the mills in which large quantities of powder (from about 0.5 to 40 kg) can be milled in a single go. Commercial attritors are usually available from Union Process, Akron, OH. The grinding medium velocity is much lower (about 0.5 m/s) than it is in Fritsch or SPEX mills and thus the energy of the attritors is comparatively lower. Attritors of different sizes and capacities are available. The grinding tanks or containers usually are either of stainless steel or stainless steel coated with alumina inside, or silicon carbide, silicon nitride, zirconia, rubber, and polyurethane. Different variety of grinding media are also available — carbide, silicon, glass, silicon, nitride, alumina, carbon steel, stainless steel, chrome steel and tungsten carbide.

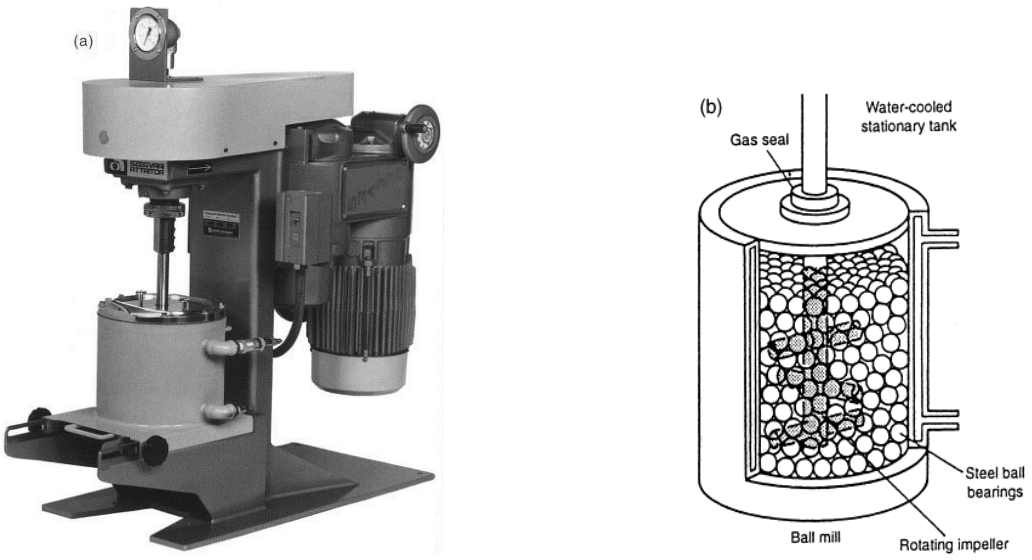

Fig. 5: Attritor mill

2.4 Process Variables:

- Mill type
- Container used for milling
- Milling speed
- Milling time
- Type, size, and size distribution of the grinding medium
- Ball-to-powder weight ratio
- Extent of filling the vial
- Atmosphere used for milling
- Process control agent
- Milling Temperature

Type of mills:

There are a different types of mills for conducting MA. These mills differ from each other in their capacity, operation speed, and their ability to exercise control on the operation by varying milling temperature and the extent of minimizing the powder contamination. Based on the powder type, their quantity, and the final composition required, a mill can be chosen suitably. Most usually, the SPEX shaker mills are used for purposes of alloy screening. Planetary ball mills are used for milling powders in large quantities. Mills are specifically designed based on their specific applications.

Milling container:

The material utilized for the processing container (granulating vessel, vial, container, or dish are a some of alternate terms used) is critical since because of effect of the grinding medium on the internal dividers of the compartment, some material will be dislodged and get joined into the powder. This can taint the powder or modify the powder composition. [14] If the material of the granulating vessel is not quite the same as that of the powder, then the powder may be contaminated with the pounding vessel material. Then again, if the two materials are the same, then the composition may be changed unless legitimate measures are taken to adjust for the extra measure of the component consolidated into the powder. Hardened steel, tool steel, hardened chromium steel, tempered steel, stainless steel, WC–Co, WC-lined steel, 18 and bearing steel are the most widely recognized sorts of materials utilized for the granulating vessels. Some particular materials are utilized for specific purposes; these incorporate copper, titanium, sintered corundum, yttria-balanced out zirconia (YSZ), incompletely settled zirconia + yttria and, sapphire and, agate, and, hard porcelain, Si3N4, and Cu–Be. The shape of the container

additionally is by all accounts vital, particularly the inner outline of the container. Both flat ended and round-finished SPEX factory compartments have been utilized. Alloying was found to happen at essentially higher rates in the flat ended vial than in the round finished container.

Milling speed:

It is easy to understand that the speedier the mill rotates the higher would be the energy transferred into the powder. At the same time, depending upon the configuration of the mill there are sure confinements to the critical rate that could be employed. For instance, in a customary ball mill expanding the rotational speed will expand the rate with which the balls move. Over a discriminating speed, the balls will be stuck to the internal walls of the vial and don't tumble down to apply any effective force. Accordingly, the most extreme pace ought to be just beneath this critical pace so that the balls tumble down from the maximum possible stature to create the most extreme impact energy. The figure below shows different types of movement of the grinding balls in the mill.

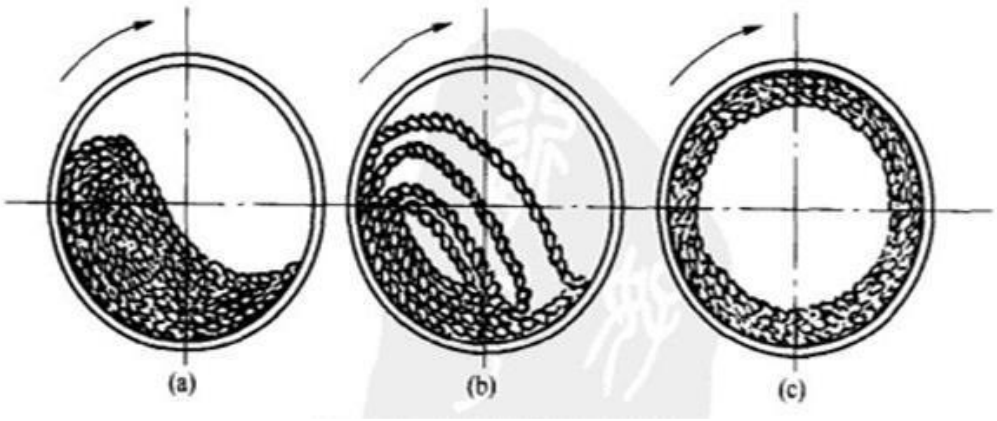

Fig. 6: Ball starts pinning to the inner wall of the vial as speed of rotation increases, and at critical speed of rotation the balls will be completely pinned to the inner walls of the vial and do not fall down to exert any impact force [16]

Another constraint to the greatest rate is that at high speeds (or intensity of processing), the temperature of the vial may achieve a high value. This may be beneficial at times where dispersion is used to advance homogenization and/or alloying in the powders. At the same time, now and again, this increment in temperature may be an impediment in light of the fact that the expanded temperature accelerates the change process and results in the decomposition of supersaturated solid solution or other metastable stages framed amid processing. Also, the high temperatures created may likewise debase the powders.

Milling time:

The milling time is the most critical parameter. Conventionally the time is so picked as to accomplish a consistent state between the cracking and cold welding of the powder particles. The milling time rely s upon the kind of mill utilized, the energy of milling, the ball-to-powder ratio, and the milling temperature. However, it ought to be understood that the level of contamination increments and some undesirable structure are formed if the powder is processed for times longer than needed. In this way, it is attractive that the powder is processed only for the optimum time and not any more [11].

Grinding medium:

Hardened steel, tool steel, hardened chromium steel, tempered steel, stainless steel, WC–Co, and bearing steel are the most well-known types of materials utilized as the granulating medium.

The density of the granulating medium ought to be sufficiently high so that the balls make enough impact on the powder. The size of the crushing medium additionally has an impact on

the processing effectiveness. A larger size (and high thickness) of the pounding medium is valuable since the bigger weight of the balls will exchange more energy to the powder particle.

Ball-to-powder weight ratio:

The proportion of the weight of the balls to the powder (BPR), sometimes alluded to as charge ratio (CR), is an imperative variable in the processing procedure. This has been differed by distinctive specialists from a quality as low as 1:1 to as high as 220:1. A proportion of 10:1 is most normally utilized while processing the powder as a part of a small capacity mill, for example, a SPEX mill. Yet, when processing is led in a substantial capacity mill, similar to an attritor, a higher BPR of up to 50:1 or even 100:1 is used [14] and [11].

The BPR has a critical impact on the time needed to attain to a specific phase in the powder being processed. The higher the BPR, the shorter is the time needed. At a high BPR, as a result of an increment in the weight extent of the balls, the quantity of collision with every unit time increments and subsequently more energy is exchanged to the powder particles thus alloying happens speedier.

Extent of filling the vial:

Since alloying among the powder particles happens because of the effect of impact forces applied on them, it is essential that there is sufficient space for the balls and the powder particles to move around unreservedly in the processing container. Accordingly, the degree of filling the vial with the powder and the balls is imperative. In the event that the amount of the balls and the powder is little, then the production rate is small. Then again, if the amount is high, then there is insufficient space for the balls to move around thus the energy of the impact is less.

Consequently, care must be taken not to fill the vial; by and large around 50% of the vial space should be left void.

Milling atmosphere:

The major impact of the processing atmosphere is on the defilement of the powder. Subsequently, the powders are processed in containers that have been either cleared or loaded with a inert gas, for example, argon or helium. High-purity argon is the most widely recognized encompassing to avert oxidation and/or contamination of the powder. [13]

Diverse environments have been utilized amid processing for particular purposes. Nitrogen or ammonia have been utilized for nitride production. Environment of Hydrogen was utilized to produce hydrides. The vicinity of air in the vial has been indicated to create oxides and nitrides in the powder, particularly if the powders are reactive in nature. Along these lines, consideration must be taken to utilize an inactive environment amid processing.

Process control agents:

The powder particles get cold-welded to each other, especially if they are ductile, due to the heavy plastic deformation experienced by them during milling. But, true alloying among powder particles can occur only when a balance is maintained between cold welding and fracturing of particles. A process control agent (PCA) (also referred to as lubricant or surfactant) is added to the powder mixture during milling to reduce the effect of cold welding. The PCAs can be solids, liquids, or gases. They are mostly, but not necessarily, organic compounds, which act as surface-active agents. The PCA adsorbs on the surface of the powder particles and minimizes cold welding between powder particles and thereby inhibits agglomeration. The surface-active agents

adsorbed on particle surfaces interfere with cold welding and lower the surface tension of the solid material. Since the energy required for the physical process of size reduction, *E* is given by Equation

$$E = \gamma . \Delta S$$

Where γ is the specific surface energy and ΔS is the increase of surface area, a reduction in surface energy results in the use of shorter milling times and/or generation of finer powders. [11]

Temperature of milling:

The milling temperature is another vital parameter in deciding the composition of the milled powder. Since there is involvement of diffusion process in the formation of alloy phases irrespective of the phase of the solid solution be it, intermetallic, nanostructure, or an amorphous phase, it is expected that the milling temperature will have a prominent effect in any of the alloy system.

Mechanism of Mechanical Alloying

During high-energy milling, the powder particles are cold welded, cracked and re-welded. At whatever point two steel balls impact, some quantity of powder is caught in the middle of them. Ordinarily, around 1000 particles with a total weight of around 0.2 mg are caught amid every impact. The impact force causes plastic deformation in the powder particles prompting work hardening and fracture. The new surfaces made to enable the particles to weld together and this prompts an increment in particle size.

Right since in the primitive phases of milling, the particles are soft (on the off chance that we are utilizing either ductile-ductile or ductile-brittle material blend), their propensity to weld together

and shape huge particles are high. A wide scope of molecule sizes builds up, 22 with some as vast as three times greater than the initial particles. The composite particles at this stage have a trademark layered structure comprising of different blends of the beginning constituents. With proceeded with distortion, the particles get work hardened and fracture by a fatigue failure mechanism and/or by the fragile flake fragmentation. Sections produced by this mechanism may keep on lessening in size without solid agglomerating powers. At this stage, the propensity to break prevails over cold welding. Because of the proceeded with effect of granulating balls, the structure of the particles is relentless, however the molecule size keeps on being the same. Hence, the between layer dividing reductions and the quantity of layers in a molecule increment [11].

In the wake of processing for a certain timeframe, unfaltering state balance is achieved when an equalization is accomplished between the rate of welding, which has a tendency to expand the normal molecule size, and the rate of breaking, which have a tendency to lessening the normal composite molecule size. Smaller particles have the capacity to withstand twisting without cracking and have a tendency to be welded into bigger pieces, with a general propensity to drive both extremely ®ne and vast particles towards a moderate size. At this stage every molecule contains significantly the majority of the beginning fixings, in the extent they were combined and the particles achieve immersion hardness because of the aggregation of strain energy. The particle size appropriation at this stage is slender, on the grounds that particles bigger than normal are lessened in size at the same rate that parts littler than normal develop through agglomeration of smaller particles

S. Torkan et. al studied the effect of milling energy on preparation of nano structured Fe70Si30 alloys. Iron in its pure form is a ferromagnetic material with low resistivity, so in a few applications it prompts huge eddy current losses. The Si addition to Fe can improve its electrical resistivity and along these lines decrease losses due to eddy currents [17]. The Fe-Si amalgams as soft magnetic materials with low coercive core, high attractive penetrability and low center losses have a huge potential for applications like electric/magnetic estimations, transformer magnets and inductor centers [18, 19]. A few examinations on Fe-Si combinations have been completed mostly for mechanical purposes including surface diffusion, quick tempering methods and uncommon schedules [20-23].

Nano-structured Fe Si based alloy has demonstrated enhanced magentic properties when its grain size is not exactly the ferromagnetic trade length which is ordinarily of the order of several tens of nanometers [24]. Mechanical alloying is a substitute method for transforming nanocrystalline compounds with specific points of interest over the fast solidification procedure. Melted alloys with high Si are exceptionally brittle. Nonetheless, ball milling method permits an extensive variety of syntheses to be mechanically alloyed for creating such a nanocrystalline compound with specific favorable circumstances over the fast hardening strategy that weakness can be overlooked whatever the silicon content is [25]. Mechanical alloying is a stochastic procedure and the quantity of variables included in the process is extensive. For a specific alloy system, the variables incorporate the mill type, speed of the granulating medium, Impact frequency, energy exchange productivity, type of processing media, ball-to-powder weight ratio (BPR), environment under which the powder is processed, purity of the powders, processing time, milling temperature, and nature and measure of the process control agents (PCA). All these have a noteworthy impact on the qualities of the processed powder. Therefore, modelling the

mechanical alloying procedure is a difficult task [26]. Modelling studies in detail have been created in past reports [27- 31]. Magini et al. [29] expected that collision is the prevailing energy exchange occasion. Distinctive milling conditions will clearly influence the route by which energy is exchanged to the processed powder and subsequently the way of last items [32, 33]. It has likewise been accounted for that stage moves in a particular framework were nearly identified with the processing conditions [34,35]. To comprehend the connection between produced phase and energy exchanged, a few examinations on account of the Fe-Zr [34], Pd-Si [35], Al-Ni [36], V-Si [37] frameworks have been finished. In every one of these examinations a basic energy to the arrangement of particular stage was distinguished.

Despite the fact that various publications have showed up as of late on the extension of solvency limit of Si in Fe through ball limit [25, 38, 39], there were no itemized studies did on the streamlining of ball milling conditions from a processing energy perspective. Further advancement obliges better comprehension of processing vitality under diverse processing parameters through portrayal of the item. Extraordinarily, count of an effectiveness variable for impact energy which prompts the final solid solution formation in this framework has not been examined yet. Additionally, correlation of processing vitality computation with the thermodynamic parts of the items development appears to be interesting. Here, the strong dissolvability expansion of Si in Fe by mechanical alloying has been examined under distinctive processing conditions. A correlation was done between the Gibbs free energy and fundamental aggregate vitality for arrangement of a supersaturated stage and the productivity of processing was assessed. The connection between impact energy and structural characteristics was explored. In addition, phase evolution with changing the aggregate energy exchange was examined.

Chapter 3
Objectives

3 Objectives

The objectives of the project are:

- Synthesis of nanostructured duplex and ferritic stainless steel from elemental Fe-Ni-Cr powder by high energy planetary milling.
- Study of phase transformation, particle size, shape and morphology of powders during planetary milling.
- Consolidation of duplex and ferritic stainless steel powder by pressureless conventional sintering.
- Determination of thermodynamic parameters during formation of stainless steel from elemental Fe-Ni-Cr powder by using Miedema Model and validation with experimental result.

Chapter 4

Experimental Procedure

4 Experimental Procedure

The elemental powder compositions of Fe–18Cr–13Ni (duplex) and Fe–17Cr–1Ni (ferrite) were selected and milled in a specially designed DDPM for 10 h under toluene atmosphere to prevent oxidation. The milling media of the DDPM consist of 600 g stainless steel balls (10 mm diameter) and ball to powder weight ratio of 6:1 was maintained during milling. The angular velocity of the supporting main shaft and jars were kept at 275 and 725 rpm respectively to attain 75 % critical speed.

Milled stainless steel powders were characterized by using X-ray diffraction (XRD) in a Philips PANalytical diffractometer using filtered Cu Kα-radiation (λ = 0.1542 nm). Williamson–Hall method was used to calculate crystal size and lattice strain of the milled powders. Morphological analysis of the milled powders was performed by scanning electron microscopy (SEM) using JEOL JSM-6480LV model.

Thermodynamic parameters (ΔS, ΔH and ΔG) of stainless steel powders for both compositions were calculated by simulation method using Miedema model. The experimental value for enthalpy of formation was calculated by using differential scanning calorimetry (DSC) Netzsch, Germany and there results were compared.

The milled powder was then compacted by using hydraulic press machine to a maximum load of 748.6 MPa. The green compact was sintered at 1000 °C with holding time of 1 hour in a tubular furnace. The sintered compact was polished using emery paper of 1/0, 2/0, 3/0 and 4/0 grades followed by cloth polishing to obtain a smooth surface for microstructural analysis.

The microstructure of the compact was analyzed using optical microscope. Hardness of the samples were also calculated by Micro hardness tester and the density of both the samples were calculated.

Table 1: Different milling parameters used

Parameter	Value
Ball to Powder weight ratio	6:1
Ball Diameter	10 mm
Grinding medium	Wet(toluene)
Weight of balls	600 gms
Milling time	30min, 2h , 5h, 10h (rest after every 30min working)
Type of mill	Dual Drive Planetary mill

Chapter 5

Results and Discussions

5 Results and Discussions

5.2 Synthesis of nano structured duplex and ferritic stainless steel powder by planetary milling

5.1.1 Milling

The XRD traces of Fe–18Cr–13Ni and Fe–17Cr–1Ni powders milled in Dual Drive Planetary mill are shown in Fig. 7(a) & (b) respectively. The duplex composition was showing ferritic phase till 2 h of milling and becomes austenite after 10 h in DDPM. This ensures that solid solution is formed after milling. Austenite phase becomes more dominant as the milling time increases. The XRD spectra consist of three peaks corresponding to γ-Fe, Cr and α-Fe respectively. This is due to the grains which are composed of large number of small regions where each plane spacing is substantially constant but differing at adjoining regions, these regions lead to occurrence of various sharp diffraction lines [40]. Here, powder particles contain grains which are bent and the non-uniform accumulated strain.

5.1.2 X-Ray diffraction study

Fig. 7 (a) and 7 (b) represents the XRD spectra of duplex and ferritic stainless steel powders milled at 0, 2, 5 and 10 h respectively in DDPM using ball to powder weight ratio of 6:1. The sharp crystalline peaks of elemental Fe, Cr and Ni start broadening continuously with milling and gradually move into the Fe lattice. It is evident from both the graphs that intensity of individual elements (Fe, Cr, Ni) decreases gradually with milling. After 10h of milling the duplex stainless steel show strong austenite peaks along with weak ferrite peaks as shown in Fig. 7 (a). In case of ferritic stainless steel, low intense austenite peaks are present along with strong ferrite peaks. Increase in milling time increases the phase transformation from α-Fe to γ-Fe and after 10h both austenite and ferrite peaks resolve in to (111) and (110) planes as shown in Fig. 7 (b). This phase transformation is due to the higher degree of defects and refinement of particles in nano-crystalline size.

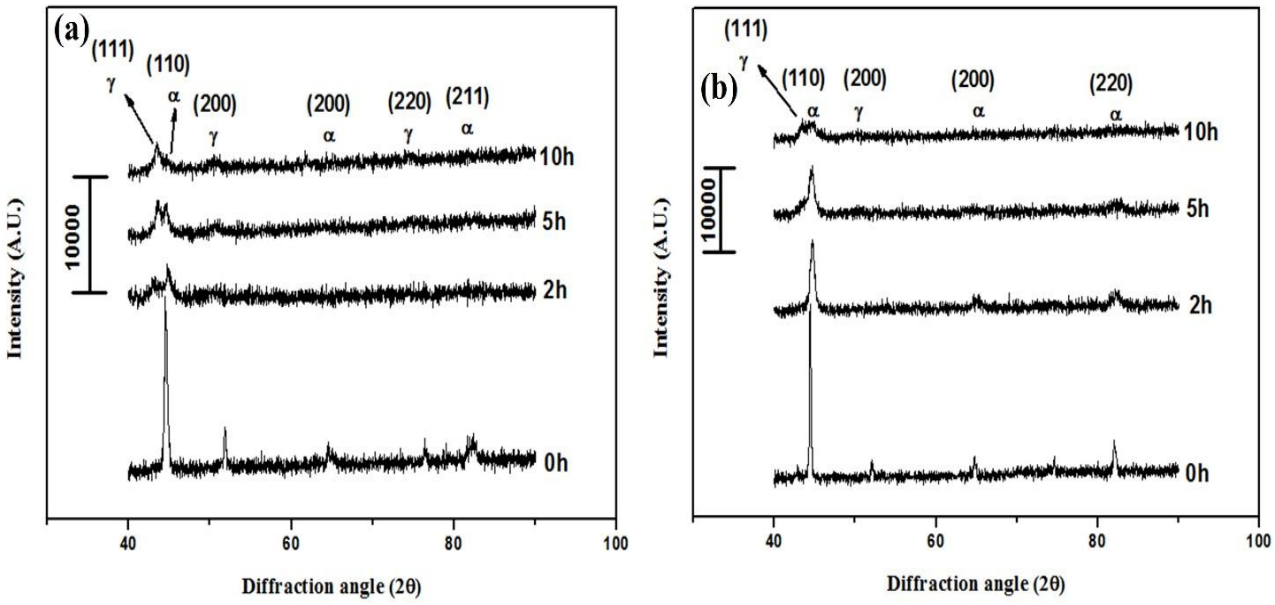

Fig. 7 XRD spectra of 0 to 10h milled (a) duplex stainless steel (b) Ferritic stainless steel powders

5.1.3 Crystallite size and lattice strain calculation

Crystal size and lattice strain of both the stainless steel are calculated using XRD data from Williamson-Hall method by de-convoluting the size and strain by calculating peak width as a function of 2θ [41]. The XRD spectra show broadening of XRD peaks with the milling time due to instrumental errors, decrease in particle size and lattice strain [42]. Crystallite size and lattice strain of duplex and ferritic stainless steel powder samples are calculated by using Williamson-Hall equation.

$$\beta cos\theta = \frac{0.94\lambda}{D} + 4\eta \sin\theta \qquad (1)$$

Where, D is crystallite size, β is full width half maxima (FWHM) and η is lattice strain.

Fig. 8 (a) and 8 (b) represent the crystallite size and lattice strain of duplex and ferritic stainless steel powder milled at 75% CS. From the figure it is clear that crystallite size decreases and strain increases with milling time due to the formation of more defects during milling. Refinement of crystallite size reaches a saturation level at higher milling time and further refinement becomes quite difficult. Due to more and more interaction of powder-ball, powder-powder and powder-jar surface, the lattice strain increases continuously even after 10h of milling. The crystallite size and strain of duplex stainless steel milled is found to be 6nm and 1.06% and that of ferritic stainless steel is 7nm and 1.03% respectively [43].

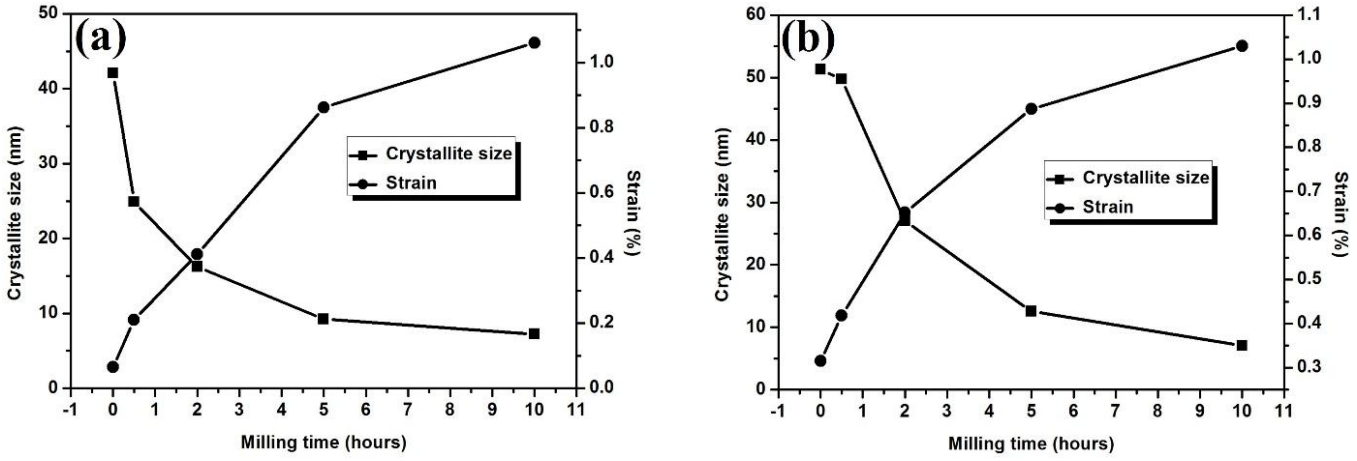

Fig. 8 Graphical representation showing the variation of crystallite size and strain at milling time of (a) duplex stainless steel (b) Ferritic stainless steel powders

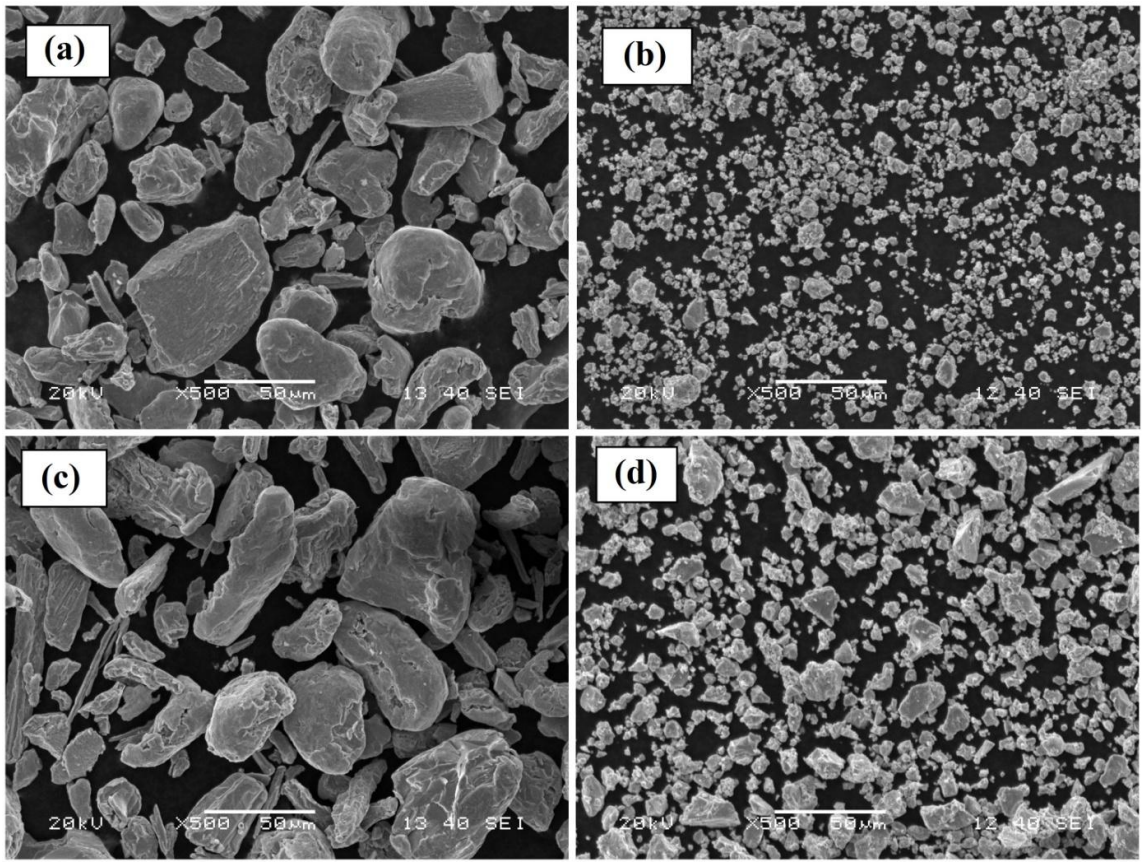

Fig. 9 SEM images of duplex stainless steel powder milled for (a) 0h (b) 10h; and ferritic stainless steel powder milled for (c) 0h (d) 10h respectively

5.1.4 Scanning electron microscopy

Fig. 9 (a) and 9 (b) depicts the SEM micrographs of 0h and 10h milled duplex stainless steel powders. Similarly, Fig. 9 (c) and 8 (d) represent SEM micrographs of ferritic stainless steel milled for 0h and 10h respectively. From the figures it is confirmed that the elemental powder particles are large and irregular in shape before milling but as milling starts particles start to form flat flakes and cold welded due to ductile nature of Fe. Finally particles are work hardened and fragmented in to smaller particles as shown the figure. This refinement of particle size reaches a saturation and further refinement of particles become more difficult after 10h.

Energy dispersive spectroscopy (EDS) analysis was carried out to study the elemental composition of stainless steel powders after 10 h of milling. Fig. 10 (a) and 10 (b) depicts the EDS spectra of duplex and ferritic stainless steel powders after 10 h of milling. From the spectra it is evident that there is no much variation in initial elemental composition and final alloy composition.

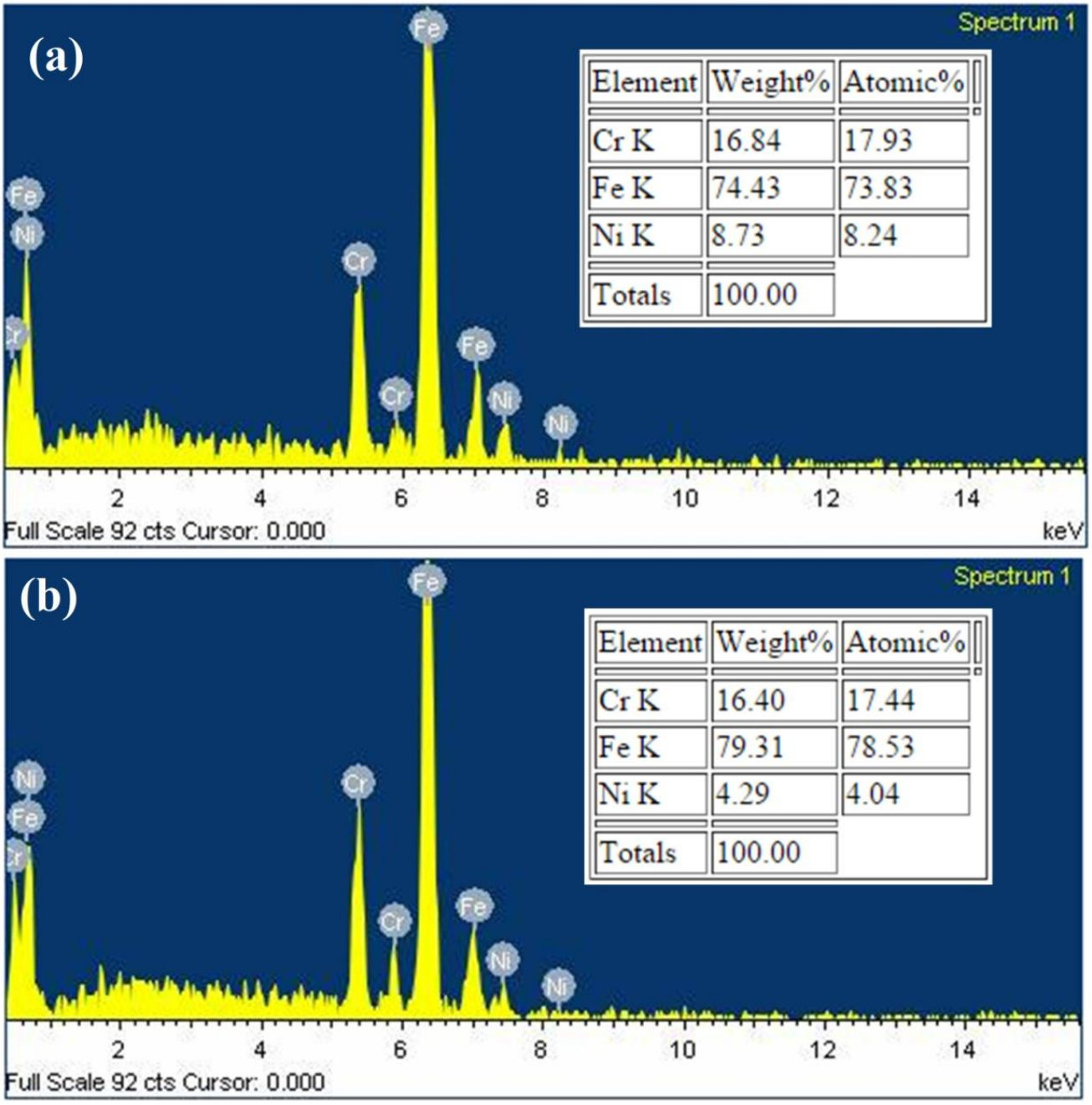

Fig. 10 EDS spectra of (a) duplex and (b) ferritic stainless steel after 10 h of milling

5.1.5 Thermal analysis

Differential scanning calorimetry (DSC) was performed by continuous heating of both duplex and ferritic stainless steel powders from 25 to 1000 °C at the heating rate of 5 °C/min under argon atmosphere. Fig 11 (a) and (b) shows the DSC graphs of duplex and ferritic stainless steel powders milled in the specially designed ball mill and it shows exothermic peaks at 677.2 and 654.5 °C respectively. The exothermic peaks represent crystal growth, lattice strain release and amorphous to crystalline phase transition during annealing with an enthalpy change of 174.90 kJ/mol and 134.2 kJ/mol in the case of duplex and ferrite respectively. Sherif E-Eskandarany and Ahmed observed exothermic peak at 1240 K with an enthalpy change of 16.88 kJ/mol for amorphous Fe74Cr18Ni8 powder prepared by rod milling after 300 h of milling [44]. Similarly, Oleszak et al. found exothermic peak at 670 °C with total heat evolved of 20–40 J/g depending on milling time for nanocrystalline duplex stainless steel powder prepared by planetary milling[8].

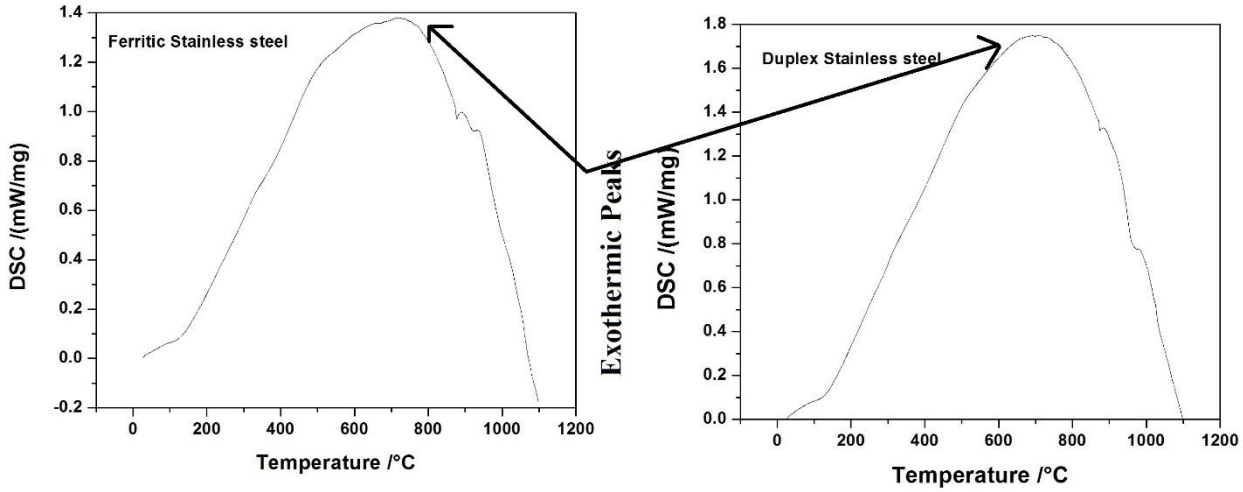

Fig. 11. DSC graphs of (a) Fe–17Cr–1Ni alloy, (b) Fe–18Cr–8Ni alloy milled in specially designed planetary ball mill after 10 h

5.1.6 Simulation Analysis

Thermodynamic analysis using Miedema model

Considering the formation of disordered A (B, C) solid solution from a mixture of pure A, B and C elements.

Here, ΔH_{ms} and ΔS_s and are the enthalpy and entropy of mixing respectively. T is the temperature at which a solid solution is formed. ΔS_s can be calculated with the assumption of configurational entropy of mixing:

$$\Delta S_s = -R(x_a lnx_a + x_b lnx_b + x_c lnx_c) \quad (2)$$

Where, x_a, x_b and x_c are mole fractions for A, B and C in the mixture.

According to Miedema semi-empirical model, the entropy of a solid solution formation consists of three terms for a ternary system:

$$\Delta S = -R(x_a lnx_a + x_b lnx_b + x_c lnx_c) \quad (3)$$

Total enthalpy for formation of solid solution is

$$\Delta H_{Total} = \Delta H_{chemical} + \Delta H_{elastic} + \Delta H_{structural} \quad (4)$$

Where, $\Delta \boldsymbol{H_{chemical}}$, $\Delta \boldsymbol{H_{elastic}}$ and $\Delta \boldsymbol{H_{structural}}$ are the chemical, elastic and structural contributions due to atomic mixing, mismatch in size and the difference in valance electrons and crystal structure of solute and solvent atoms, respectively. The complete form of $\Delta \boldsymbol{H_{chemical}}$ is as follows:

$$\Delta \boldsymbol{Hchemical} = \frac{2f(C^S)(X_A V_A^{\frac{2}{3}} + X_B V_B^{2/3})*[\text{-P}(€)^2 + Q(\Delta n_{ws})^{2/3}]}{(n_{ws}^A)^{-1/3} + (n_{ws}^B)^{-1/3}} \quad (5)$$

Where $\boldsymbol{X_a}$ and $\boldsymbol{X_b}$ are the mole fractions of elements A and B; €, *V* and n_{ws} are work function, molar volume and electron density of constituents, respectively. *P* and *Q* are empirical constants and f(C^s) is the concentration function that for solid solution is given by

$$f(C^S) = C_A^S . C_B^S \quad (6)$$

$$C_A^S = \left(\frac{X_A V_A^{\frac{2}{3}}}{X_A V_A^{\frac{2}{3}} + X_B V_B^{\frac{2}{3}}} \right) \quad (7)$$

$$C_B^S = \left(\frac{X_B V_B^{\frac{2}{3}}}{X_A V_A^{\frac{2}{3}} + X_B V_B^{\frac{2}{3}}} \right) \quad (8)$$

$$\Delta H_{elastic} = x_b \Delta E_{A\ in\ B} + x_a \Delta E_{B\ in\ A} \quad (9)$$

Where $\Delta E_{A\ in\ B}$ and $\Delta E_{B\ in\ A}$ are the elastic energy caused by dissolving A in B and B in A, respectively and can be estimated by

$$\Delta \boldsymbol{Ea\ in\ b} = \frac{2K_a . G_b . (\Delta V)^2}{3K_a V_b + 4G_b V_a} \quad (10)$$

$$\Delta \boldsymbol{Eb\ in\ a} = \frac{2K_b . G_a . (\Delta V)^2}{3K_b V_a + 4G_a V_b} \quad (11)$$

Table 2. Values of different parameters for Fe, Ni and Cr

	Fe	Cr	Ni
Molar Volume ($V^{2/3}$), (cm^2)	3.7	3.7	3.5
Electron density ($n_{ws}^{1/3}$), $(d.u.)^{1/3}$	1.77	1.73	1.75
Work function (€), (V)	4.93	4.65	5.2
K (GPa)	170	160	180
G (GPa)	82	115	76

Where $\Delta \boldsymbol{E}_{A\ in\ B}$ and $\Delta \boldsymbol{E}_{B\ in\ A}$ are the elastic energy caused by 'A' dissolving in 'B' and 'B' dissolving in 'A' respectively. Where K and G are bulk and shear modulus respectively.

$\Delta S_{structural}$ was neglected as the value is negligible compared to other two enthalpies.

Table 2 shows the list of various parameters used for Fe, Cr and Ni.

Gibb's free energy for formation of solid solution was calculated by using the following equation:

$$\Delta G = \Delta H_{Total} - T\Delta S \qquad (12)$$

Here temperature 'T' for formation of solid solution is assumed 300K.

Table 3 shows the value of different thermodynamic parameters calculated using Miedema model. It is observed from the table that ΔG for duplex stainless steel is higher than ferritic stainless steel. The reason is due to diffusion of higher amount of alloying element in duplex steel than ferritic steel.

Table 3 Values of thermodynamic parameters calculated using Miedema model

	ΔH (kJ/mol)	ΔS (J/mol)	ΔG (kJ/mol)
Duplex	-14.32	6.93	-16.39
Ferrite	-2.81	4.35	-4.12

Table 4 Comparative study of theoretical and experimental values for enthalpies of duplex and ferritic stainless steel

	ΔH (kJ/mol)[theoretical]	ΔH (kJ/mol)[experimental]
Duplex SS	-14.32	-174.9
Ferritic SS	-2.81	-134.2

5.3 Analysis of consolidated compact

5.2.1 Microstructure analysis.

Fig. 12 shows optical micrographs of duplex and ferritic stainless steel samples consolidated at 1000°C for 1 h. The micrographs show the presence of stainless steel particles and pores. At higher temperature austenite phase become more stable. Whereas ferritic stainless steel shows more of ferrite phase due to absence or minimal presence of austenite stabilizer i.e. Ni.

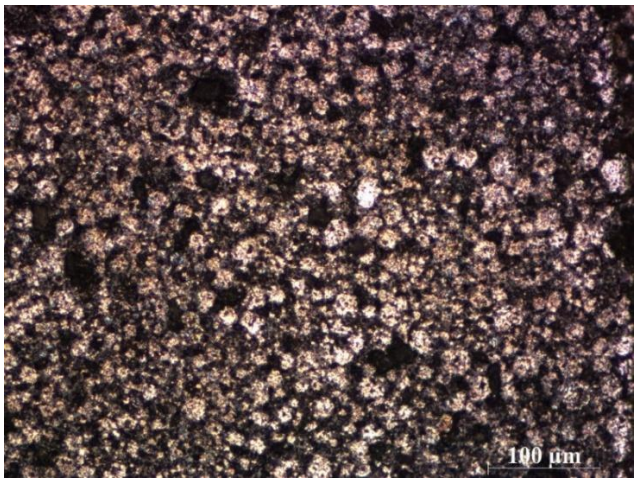

(a)

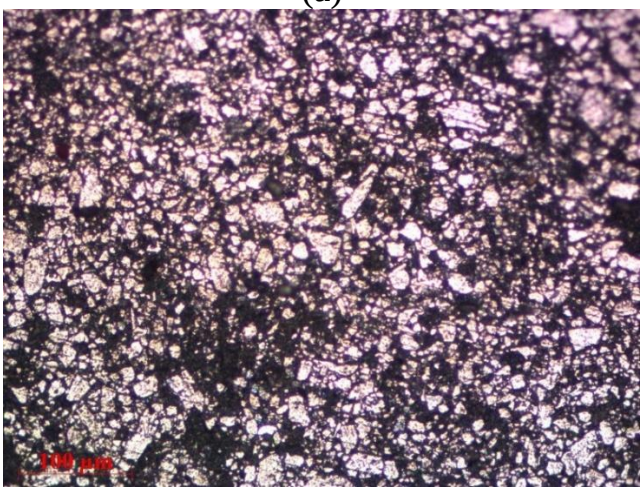

(b)

Fig. 12 Optical microstructure of (a) duplex stainless steel and (b) ferritic stainless steel samples sintered at 1000°C for1 h.

5.2.2 SEM Analysis

Fig. 13 (a) and (b) shows the SEM micrographs ferritic and duplex stainless steel. Similarly, Fig. 13 (c) and (d) shows the SEM micrographs of 1 wt. % yittria dispersed ferritic and duplex stainless steel. From the initial SEM analysis of the compacted powder it is evident that the particles were initially small in shape and segregated with large inter-particle distances but later after compaction and sintering, the mean inter-particle distance decreases and the particle size increases.

Energy dispersive spectroscopy (EDS) analysis was carried out to study the elemental composition of stainless steel compacts after consolidation. Fig. 14 depicts the EDS spectra of 1 wt. % yittria dispersed ferritic stainless steel compact after sintering at 1000°C. Table 5 shows the quantitative value of different elements present in yittria dispersed ferritic stainless steel. From the table it is evident that there is no much variation in initial elemental composition and final alloy composition.

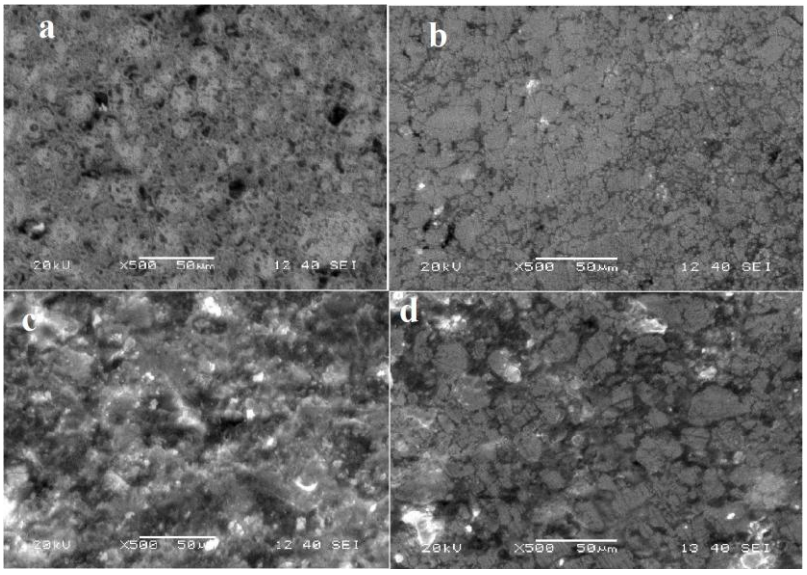

Fig. 13 SEM images of compacted powders of (a) duplex (b) ferritic stainless steel and 1 wt. %Yittria strengthened (c) Duplex and (d) ferritic stainless steel

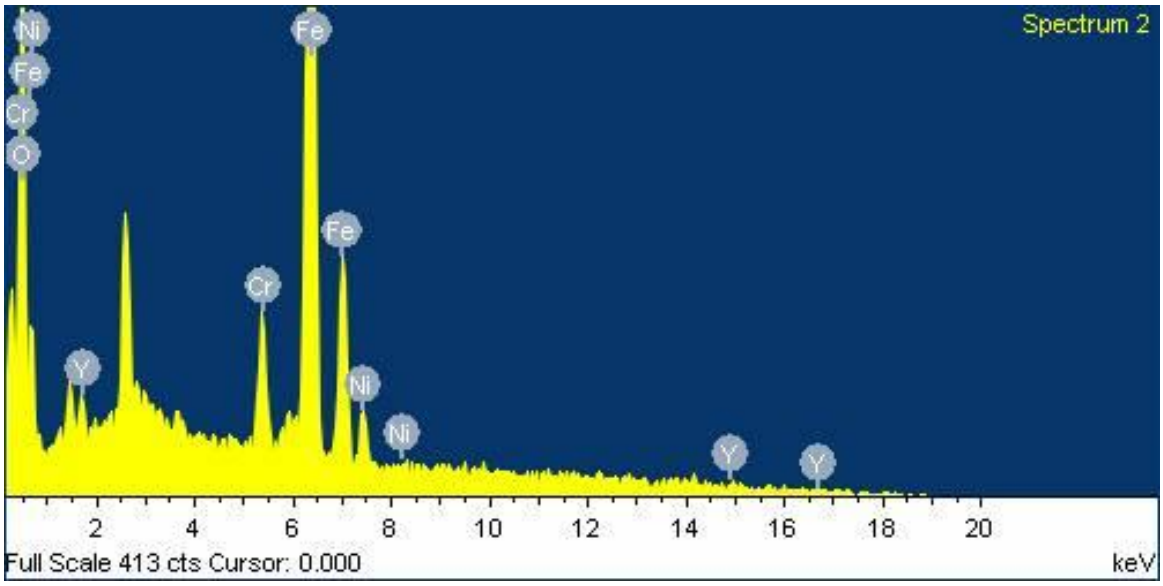

Fig. 14: EDS spectra of 1wt. % Yittria dispersed ferritic stainless steel

Table 5: Elemental composition of 1wt. % yittria dispersed ferritic stainless steel

Element	**Wt. %**	**Atomic %**
O	18.75	44.62
Cr	4.29	3.14
Fe	71.58	48.79
Ni	5.21	3.38
Y	.16	.07

5.2.3 Density and hardness study

Maximum densities of 63 to 67% were achieved in all four types of stainless steel samples sintered at 1000 °C. Average hardness values of duplex and ferritic stainless steels at 1000 °C are around 257 HV and 225 HV respectively and the values obtained are high compared with previous literatures [45, 46]. There is variation in hardness with indentation load and it is due to indentation size effect (ISE). ISE is caused due to the surface effect; strain gradient effect and mechanism of non-dislocation based on mass transport due to point defects [47]. This effect which have a direct relation with the intrinsic structural factors of the materials like indentation elastic recovery, work hardening during indentation, as well as surface dislocation pining [48,

49]. The similar phenomena of duplex and ferritic stainless steels have been explained by Shashanka et al [42]. Density and hardness of duplex and ferritic stainless steel are tabulated in Table 6.

Table 6. Density and hardness value of duplex and ferritic stainless steel sample sintered at 1000°C

	Density (g/cm^3)			Vickers Micro-hardness (HV)		
	Theoretical	Experimental	Sintered (%)	10gf	25gf	50gf
Duplex	7.84	5.18	66.07	263	257	250
Ferrite	7.75	4.87	62.84	251	212	210
Duplex(1wt.%Y_2O_3)	7.81	5.20	66.58	306	254	212
Ferritic(1wt.%Y_2O_3)	7.72	5.03	65.15	225	211	170

Chapter 6
Conclusions

6 Conclusions:

The basic conclusions that can be drawn from the experimental results are given below:

- Nano-structured duplex and ferritic stainless steel can be synthesized from elemental Fe-Ni-Cr powder by high energy planetary milling.
- The ferritic phase transformed to duplex phase in case of duplex stainless steel after 10 hours of milling.
- The crystallite size of duplex and ferritic stainless steel decreases from 43 to 6 nm and from 52 to 7nm respectively. Similarly, the lattice strain increases from 0.06 to 1.06 % in case of duplex and from 0.32 to 1.03 % in case of ferritic stainless steel respectively.
- The shape of the powder particles changes from irregular to spherical as the milling proceeds.
- The experimental value for enthalpy of formation of duplex and ferritic steels were calculated to be 134.2 and 174.9 respectively which is different from their theoretically calculated values. This shows the dependency of enthalpy of formation of duplex and ferritic stainless steel on various other milling parameters such as well. They may be milling speed, milling atmosphere, type of mill etc.

Chapter 7

Future Scope

7 Future Scope

- As can be seen that enthalpy of formation is a function of some others milling parameters as well therefore a comparative study of different milling parameters with their enthalpies of formation can be done to get a suitable relationship between various milling parameters and their enthalpy of formation.

- Values of various other thermodynamic parameters such as ΔS and ΔG can be calculated by experimental methods and their comparative study can be done with their theoretical counterparts. This may help in establishing relation between them.

- Extent of phase transformation as a function of different milling parameters can be studied.

8 References:

[1] S. Pasebani, I. Charit, Y.Q. Wu, D.P. Butt, J.I. Cole, Mechanical alloying of lanthana bearing nanostructured ferritic steels, Acta Mater. 61 (2013) 5605–5617.

[2] K.J. Kurzydłowski, Microstructural refinement and properties of metals processed by severe plastic deformation, Bull. Pol. Acad. Sci. Tech. Sci. 52 (2004) 275.

[3] T. Tanaka, K.N. Ishihara, P.H. Shingu, Formation ofmetastable phases of Ni–C,Metall. Trans. A. 23 (1992) 2421.

[4] M.J. Tracy, J.R. Groza, Nanophase structure in Nb rich-Nb3Al alloy by mechanical alloying, Nanostruct. Mater. 1 (1992) 369.

[5] M.A. Meyers, A.Mishra, D.J. Benson,Mechanical properties of nanocrystalline materials, Mater. Sci. 51 (2006) 427–556.

[6] S.D. Kaloshkin, V.V. Tcherdyntsev, I.A. Tomilin, Yu.V. Baldokhin, E.V. Shelekhov, Phase transformations in Fe–Ni system at mechanical alloying and consequent annealing of elemental powder mixtures, Physica B 299 (2001) 236–241.

[7] M.H. Enayati, M.R. Bafandeh, Phase transitions in nanostructured Fe–Cr–Ni alloys prepared by mechanical alloying, J. Alloys Compd. 454 (2008) 228–232.

[8] D. Oleszak, A. Grabias, M. P˛ekała, A. Swiderska-Sroda, T. Kulik, Evolution of structure in duplex steel powders during ball milling and subsequent sintering, J. Alloys Compd. 434–435 (2007) 340–343.

[9]. K.J. Kurzydłowski, Microstructural refinement and properties of metals processed by severe plastic deformation, Bull. Pol. Acad. Sci. Tech. Sci. 52 (2004) 275-277.

[10] Turker M, Karatas C, Saritas S. Computation of flow behaviors of mechanically alloyed and turbola processed powder PIM feedstock by capillar rheometer.

[11] C. Suryanarayana, Mechanical alloying and milling (2001)

[12] M.O. Lai, L. Lu, Mechanical Alloying, 1998.

[13] B.S. Murty, S. Ranganathan, Int. Mater. Rev. (1998).

[14] C. Suryanarayana, Prog. Mater. Sci. 46 (2000).

[15] C. Suryanarayana (Ed.), Non-equilibrium Processing of Materials, Pergamon Press, Oxford, 1999.

[16] Kilinc Y, Turker M, Saritas S. Investigation of the mechanical properties of iron based super alloys produced by mechanical alloying techniques

[17] A.H. Bahrami, S.Sharafi, H. Ahmadian Baghbaderani, The effect of Si addition on the microstructure and magnetic properties of Permalloy prepared by mechanical alloying method, J. Adv. Powder. Technol. 24 (2013) 235-241.

[18] Y. Yoshizawa, Y. Bizen, S. Arakawa, Magnetic properties of Fe-Cu-Nb-Si-B nanocrystalline alloys with low magnetostriction, J. Mater. Sci. Eng. 181 (1994) 871-875.

[19] R.C. O'handley, Modern Magnetic Materials: Principles and Applications, Wiley New York, 2000 .

[20] T. Ros-Yanez, Y. Houbaert, M. De Wulf, Evolution of magnetic properties and microstructure of high-silicon steel during hot dipping and diffusion annealing, IEEE. T. Magn, 38 (2002) 3201-3203.

[21] L. Varga, F .Mazaleyrat, J. Kovac, J. Greneche, Structural and magnetic properties of metastable $Fe_{1-x}Si_x$ ($0.15< x< 0.34$) alloys prepared by a rapid-quenching technique, J. Phys. Condens. Mat, 14 (2002) 1985.

[22] N. H. Heo, Cold rolling texture, nucleation and direction distribution of {110} grains in 3% Si-Fe alloy strips, Mater. Lett, 59 (2005) 2827–2831.

[23] X. Fang, Y. Liang, F. Ye, J. Lin, Cold rolled Fe-6.5 wt.% Si alloy foils with high magnetic induction, J. Appl. Phys. 111 (2012) 094913-094914.

[24] G. Herzer, Grain size dependence of coercivity and permeability in nanocrystalline ferromagnets, IEEE. T. Magn, 26 (1990) 1397-1402.

[25] R. Rodríguez, G. Pérez Alcázar, H. Sánchez, J. Greneche, Milling time effects on the magnetic and structural properties of the $Fe_{70}Si_{30}$ system, Microelectr. J. 39 (2008) 1311-1313.

[26] C. Suryanarayana, Mechanical alloying and milling, Prog. Mater. Sci. 46 (2001) 145-147.13

[27] T. Courtney, Process Modeling of mechanical alloying (overview), Mater. T. JIM. 36 (1995) 110-122.

[28] T. Iwasaki, T.Yabuuchi, H. Nakagawa, S. Watano, Scale-up methodology for tumbling ball mill based on impact energy of grinding balls using discrete element analysis, J. Adv. Powder. Technol. 21 (2010) 623-629.

[29] M. Magini, A. Iasonna, Energy transfer in mechanical alloying (overview), Mater. T. JIM. 36 (1995) 123-133.

[30] C. Koch, Research on metastable structures using high energy ball milling at North Carolina State University (overview), Mater.T. JIM. 36 (1995) 85-95.

[31] R. Watanabe, H. Hashimoto, G.G. Lee, Computer simulation of milling ball motion in mechanical alloying (overview), Mater.T. JIM. 36 (1995) 102-109.

[32] B. Murty, M. Mohan Rao, S. Ranganathan, Milling maps and amorphization during mechanical alloying, Acta. Metal. Mater. 43 (1995) 2443-2450.

[33] H. Zhang, X. Liu, Analysis of milling energy in synthesis and formation mechanisms of molybdenum disilicide by mechanical alloying, Int. J. Refract. Met. H. 19 (2001) 203-208.

[34] N. Burgio, A. Iasonna, M. Magini, S. Martelli, F. Padella, Mechanical alloying of the Fe−Zr system. Correlation between input energy and end products, II. Nuovo. Cimento. D. 1991, pp. 459-476.

[35] F. Padella, E. Paradiso, N. Burgio, M. Magini, S. Martelli, W. Guo, A. Iasonna, Mechanical alloying of the Pd-Si system in controlled conditions of energy transfer, J. Less commen. Met. 175 (1991) 79-90.

[36] M. Ragab, H. G. Salem, Effect of milling energy on the structural evolution and stability of nanostructured Al-5.7 wt.% Ni mechanically alloyed eutectic alloy, Powder. Technol. 222 (2012) 108-116.14

[37] L. Liu, L. Lu, M. Lai, M. Magini, G. Fei, L. Zhang, Different Pathways of Phase Transition in a V–Si System Driven by Mechanical Alloying, Mater. Res. Bull. 33 (1998) 539-545.

[38] M. Kalita, A. Perumal, A. Srinivasan, Structure and magnetic properties of nanocrystalline $Fe_{75}Si_{25}$ powders prepared by mechanical alloying, J. Mag. Mag. Mater. 320 (2008) 2780-2783.

[39] J. Ding, Y. Li, L. Chen, C. Deng, Y. Shi, Y. Chow, T. Gang, Microstructure and soft magnetic properties of nanocrystalline Fe–Si powders, J. Alloy. Compd. 314 (2001) 262- 267.

[40] B.D. Cullity, S.R. Stock, Elements of X-Ray Diffraction, Pearson, 2003. (Paperback, ISBN-13: 9780131788183).

[41] R. Shashanka, D. Chaira, Phase transformation and microstructure study of nano structured duplex and ferritic stainless steel powder prepared by planetary milling, Powder Technol. 259 (2014) 125–136.

[42] R. Shashanka, D. Chaira, Development of nano-structured duplex and ferritic stainless steel by pulverisette planetary milling followed by pressureless sintering, Mater Charact. (2014), doi: 10.1016/j.matchar.2014.11.030.

[43] Shalabh Gupta, R. Shashanka, D. Chaira, Synthesis of nano-structured duplex and ferritic stainless steel powders by planetary milling: An experimental and simulation study

[44] M. Sherif E-Eskandarany, H.A. Ahmed, Morphology and structural studies of amorphous of Fe74Cr18Ni8 alloy prepared by the rod-milling technique, J. Alloys Compd. 216 (1994) 213 220

[45] Duyi Ye, Investigation of cyclic deformation behaviour in the surface layer of 18Cr– 8Ni duplex stainless steel based on Vickers microhardness measurement, Mater. Chem. Phys. 93 (2005) 495–503.

[46] S. Picard, J.B. Memet, R. Sabot, J.L. Grosseau-Poussard, J.P. Riviere, R. Meilland, Corrosion behavior, microhardness and surface characterisation of low energy, high current ion implanted duplex stainless steel, Mater. Sci. Eng. A 303 (2001) 163–172.

[47] Ilze Manika, Janis Maniks, Size effects in micro- and nanoscale indentation, Acta Mater. 54 (2006) 2049–2056.

[48] Jianghong Gong, Wu. Jianjun, Zhenduo Guan, Examination of the indentation size effect in low-load Vickers hardness testing of ceramics, J. Eur. Ceram. Soc. 9 (1999) 2625–2631.

[49] I.H. Bueckle, Use of the hardness test to determine other material properties, in: J.H. Westbrook, H. Conrad (Eds.), The Science of Hardness Testing and Its Research Application, American Society for Metals, Metal Park, OH, 1973, pp. 453–494